Supporting Information

Improving the Optoelectronic Properties of Single-Crystal Antimony Sulfide Rods through Simultaneous Defect Suppression and Surface Cleaning

Xiaohui Liu [a], Shunhong Dong [a], Xiaolu Zheng [a], Yicheng Zhang [b], Yuan Yao [c], Weibin Zhang [a], Zhiyong Liu [a], Ting Zhu [a], Hong-En Wang [a,*]

[a] College of Physics and Electronic Information, Yunnan Key Laboratory of Optoelectronic Information Technology, Key Laboratory of Advanced Technique & Preparation for Renewable Energy Materials, Ministry of Education, Yunnan Normal University, Kunming 650500, China.

[b] College of Chemistry and Chemical Engineering, Yunnan Normal University, 650500 Kunming, China.

[c] Beijing National Laboratory of Condensed Matter Physics, Institute of Physics, Chinese Academy of Sciences, Beijing 100190, China.

* Correspondence: hongen.wang@outlook.com; hongen.wang@ynnu.edu.cn

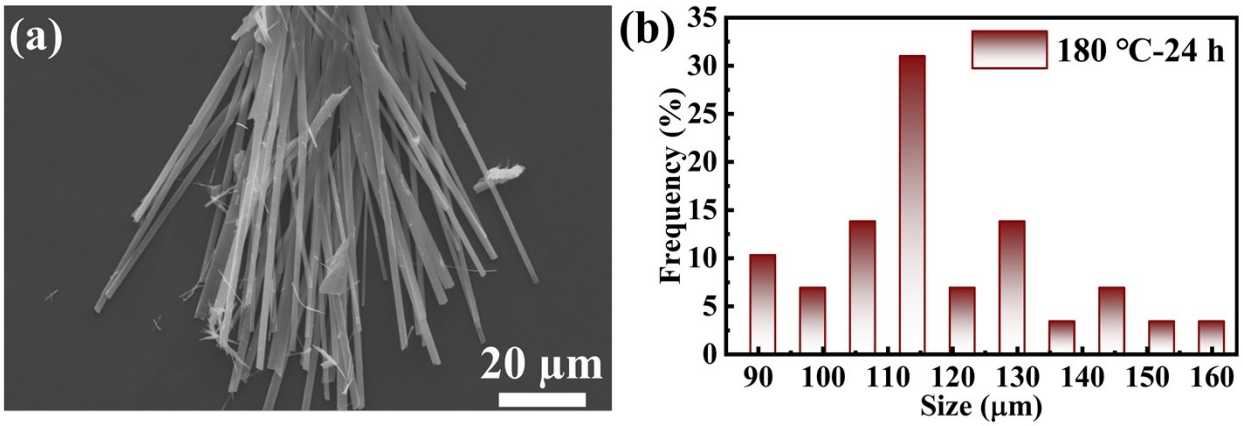

Figure S1. A representative low-magnification SEM image of pristine Sb_2S_3 (p-Sb_2S_3) rods obtained by hydrothermal reaction at 180 ℃ for 24 h.

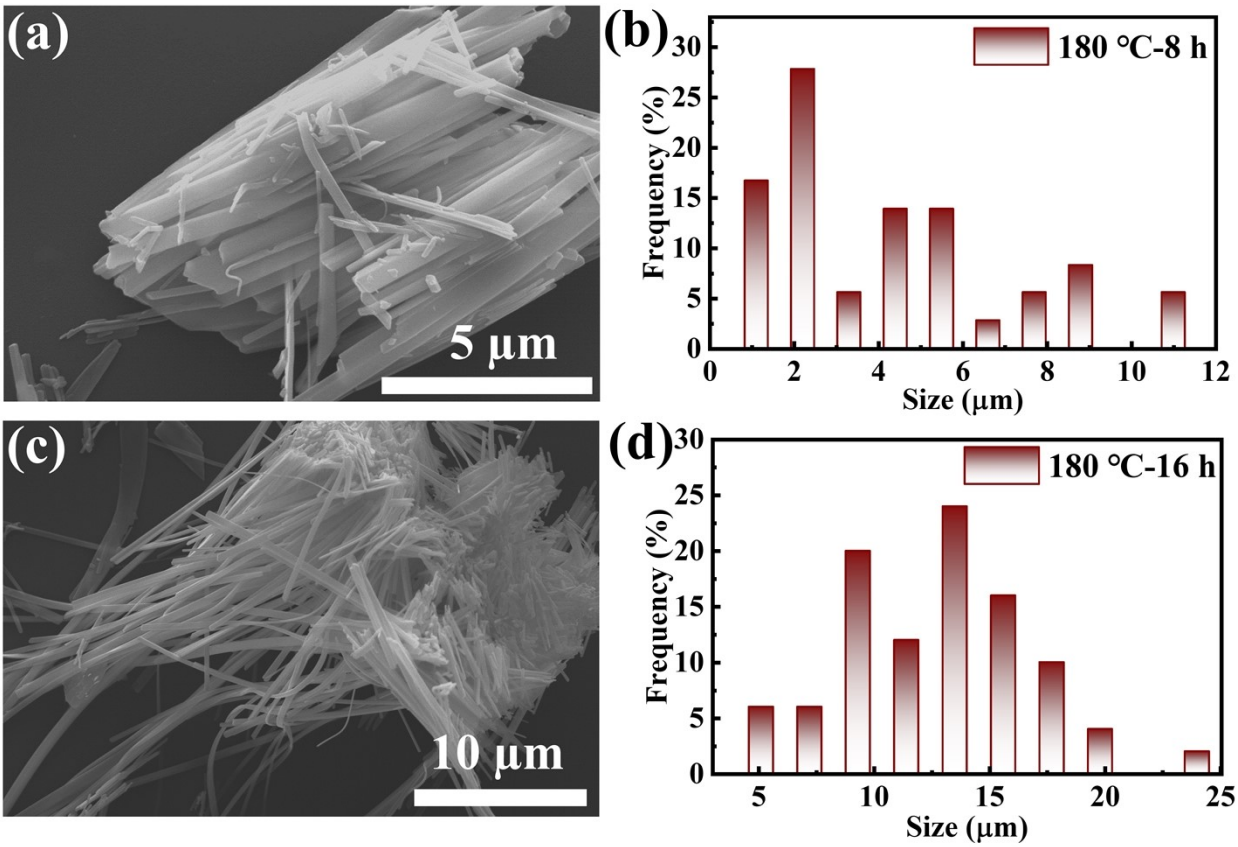

Figure S2. (a, c) SEM images and (b, d) corresponding size distribution histograms of the Sb_2S_3 rods prepared by hydrothermal reactions at 180 ℃ for (a, b) 8 h and (c, d) 16 h, respectively.

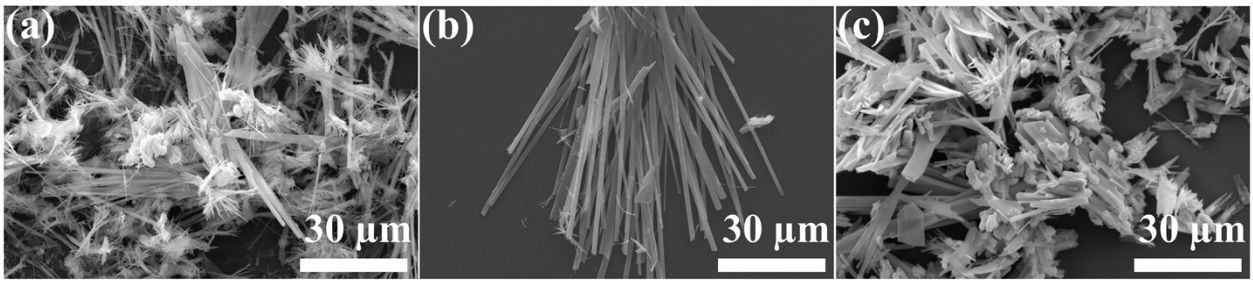

Figure S3. SEM images of the Sb_2S_3 rods hydrothermally synthesized at (a) 160 °C, (b) 180 °C, and (c) 200 °C for 24 h, respectively.

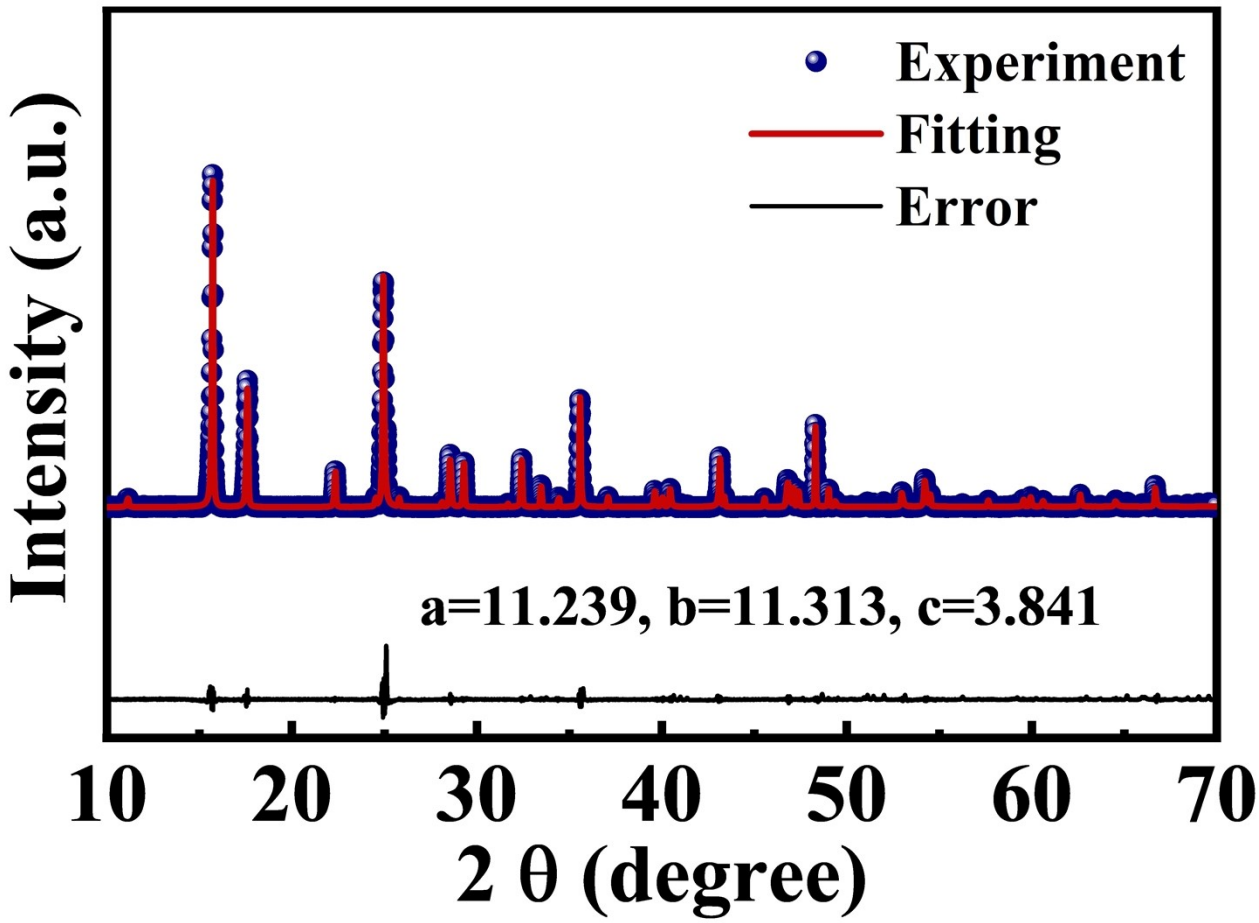

Figure S4. Rietveld refinement analysis for the XRD pattern of the Sb_2S_3-H_2/Ar sample.

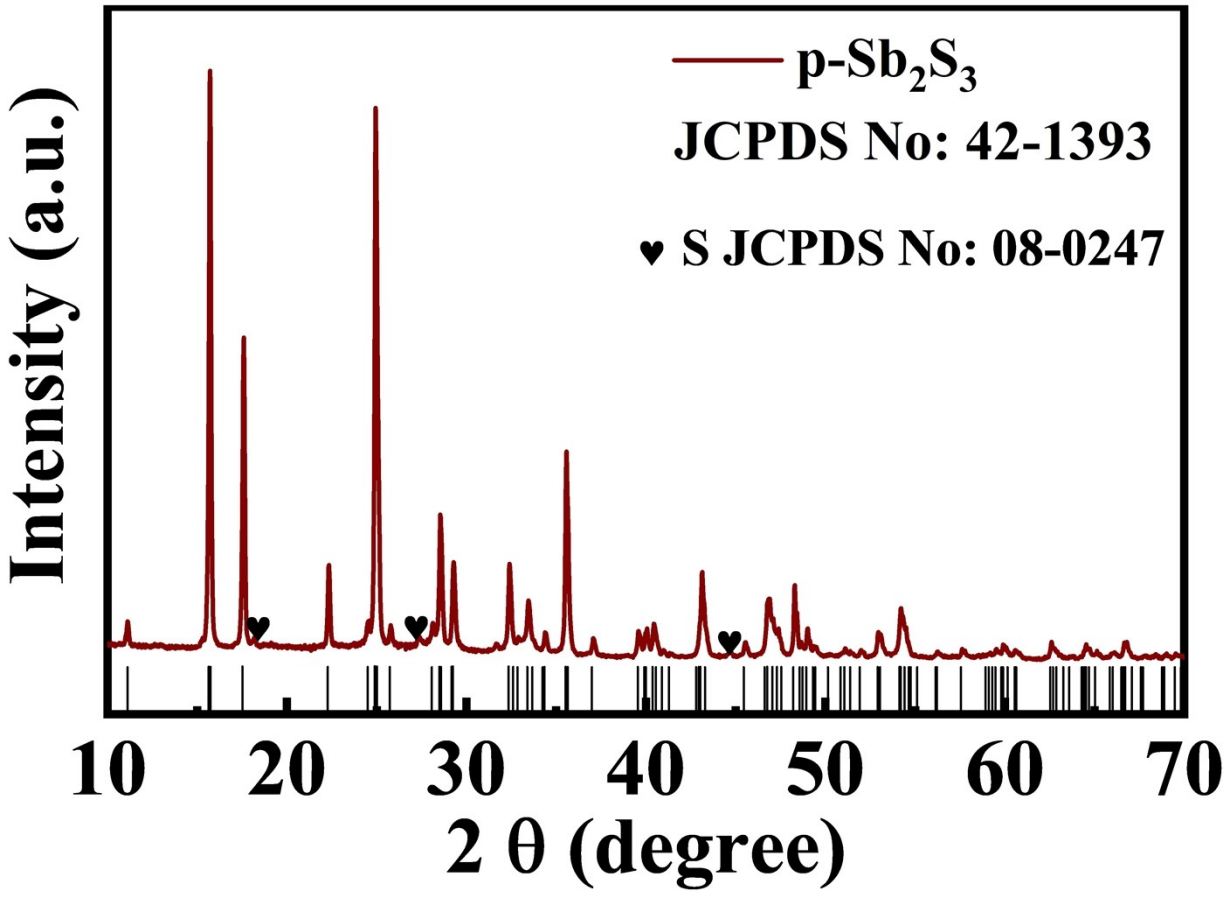

Figure S5. XRD pattern of the hydrothermally prepared pristine Sb_2S_3 rods (p-Sb_2S_3) containing trace sulfur impurity.

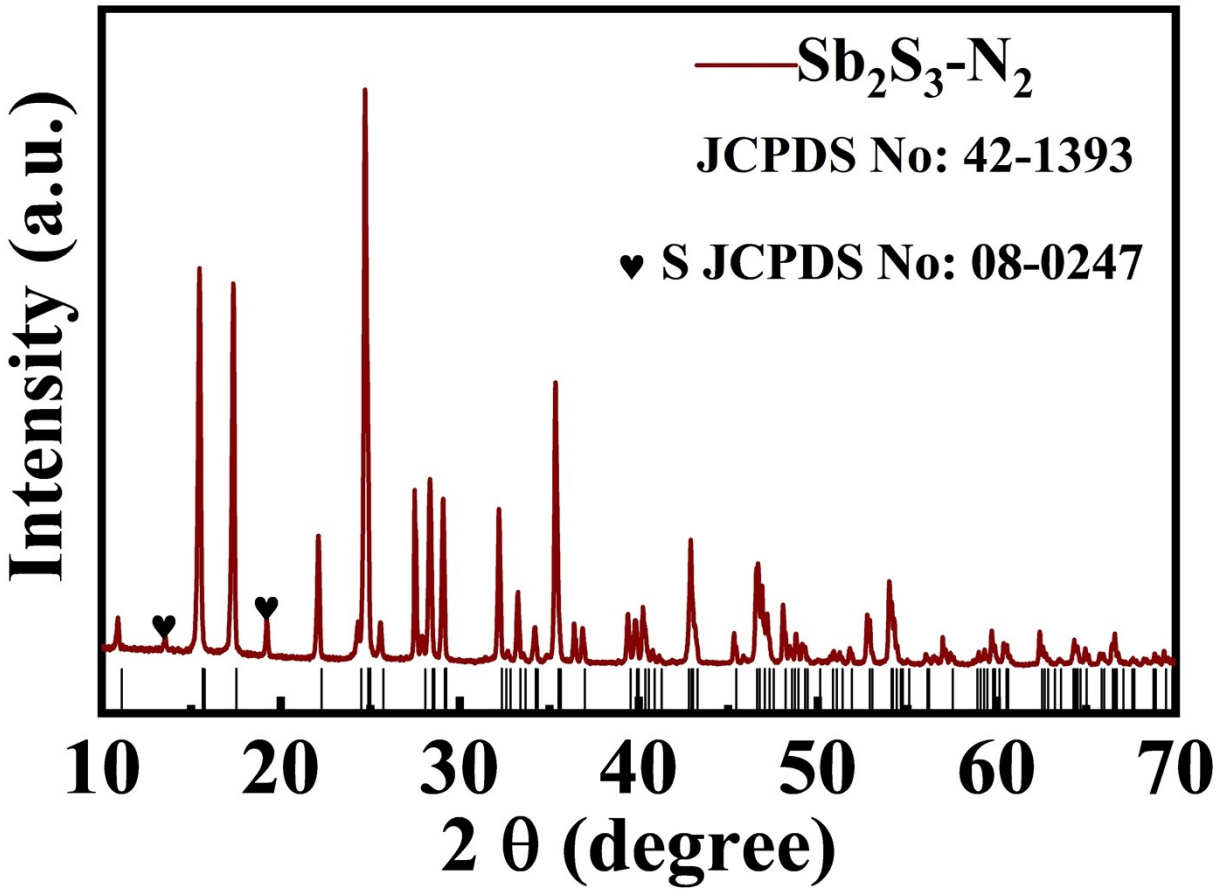

Figure S6. XRD pattern of the hydrothermally prepared pristine Sb_2S_3 rods followed by annealing in nitrogen (Sb_2S_3-N_2) containing residual sulfur impurity.

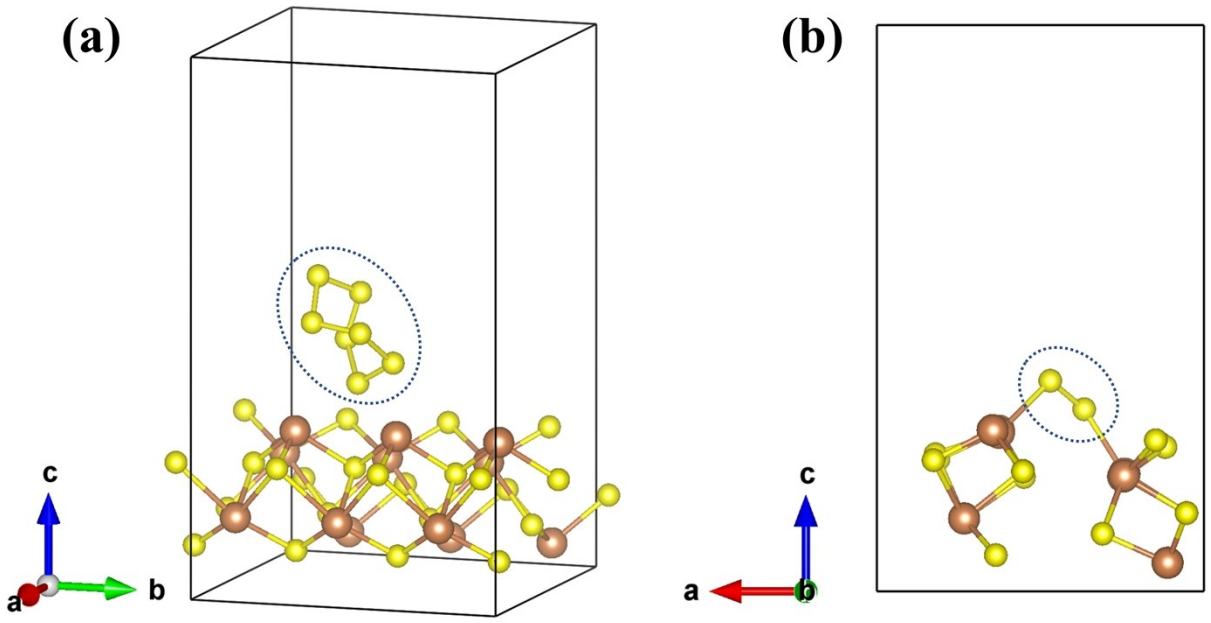

Figure S7. Adsorption configurations of one (a) S_8 and (b) S_2 molecule on Sb_2S_3 (010) surface after geometry optimization, leading to an adsorption energy of -0.69 and -1.22 eV, respectively. The S_8 (left) and S_2 (right) molecules have been marked by dotted ellipses for clarity.

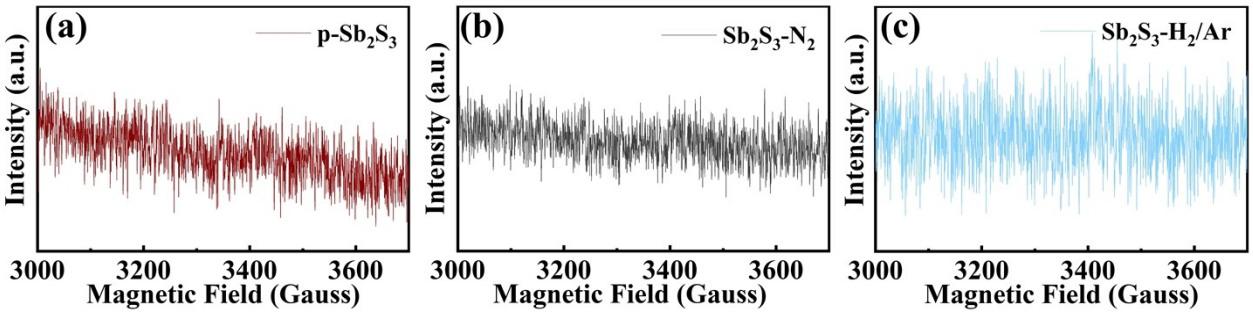

Figure S8. EPR spectra of the (a) p-Sb_2S_3, (b) Sb_2S_3-N_2, and (c) Sb_2S_3-H_2/Ar samples.

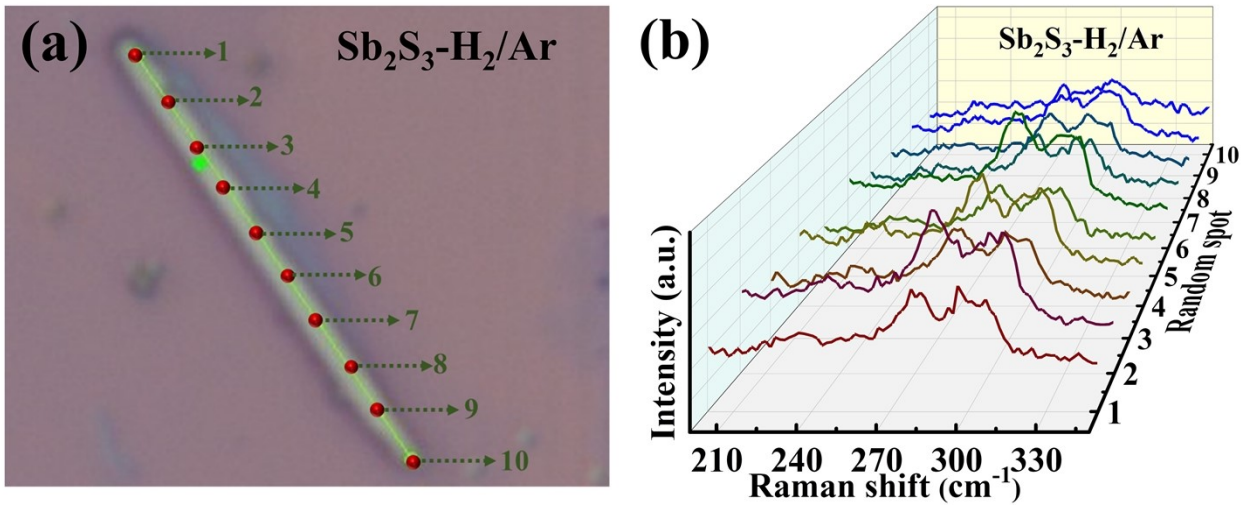

Figure S9. Linear sweep Raman spectra of (b, right) a single Sb_2S_3-H_2/Ar rod at several different positions (a, left).

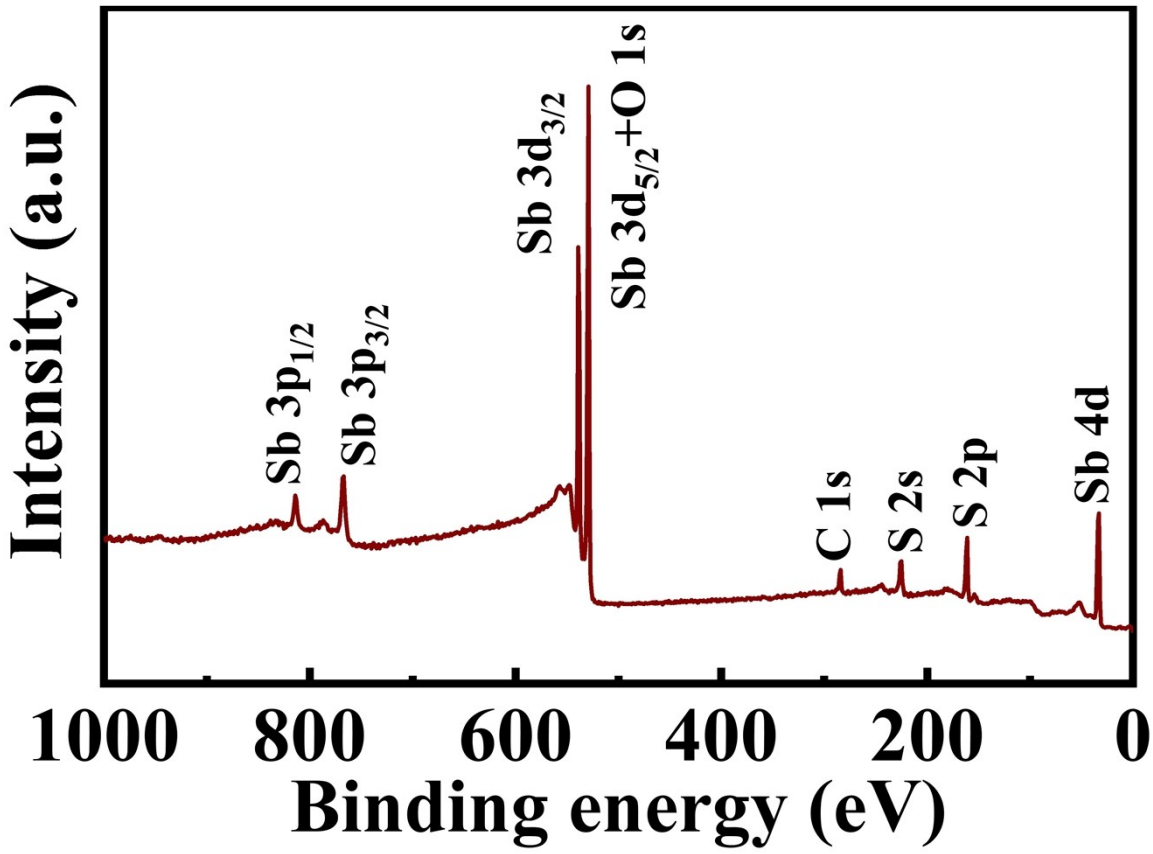

Figure S10. Survey XPS spectrum of the Sb_2S_3-H_2/Ar sample.

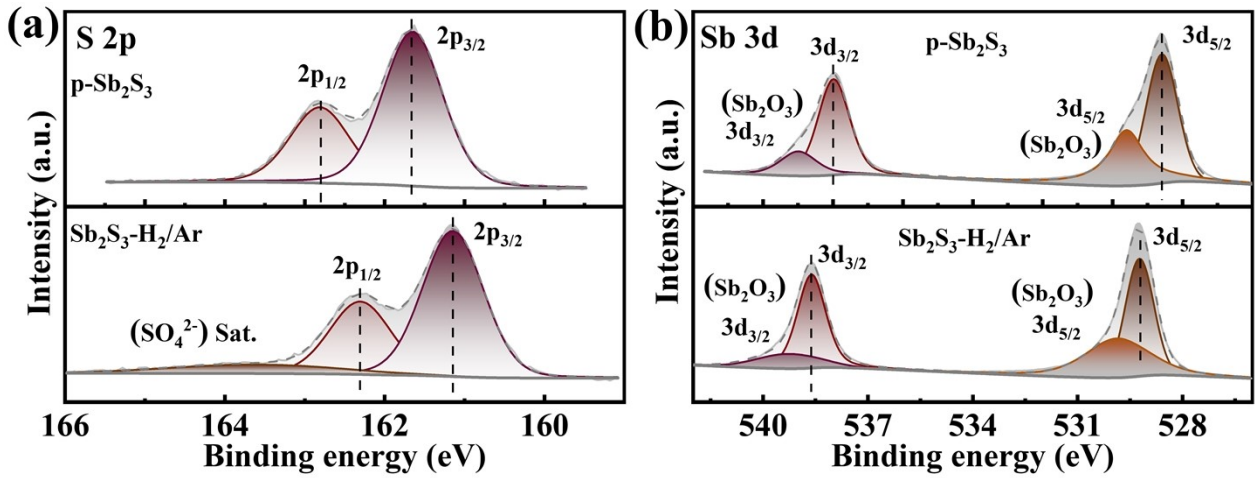

Figure S11. High-resolution XPS spectra of (a) S 2*p* and (b) Sb 3*d* of p-Sb_2S_3 and Sb_2S_3-H_2/Ar samples.

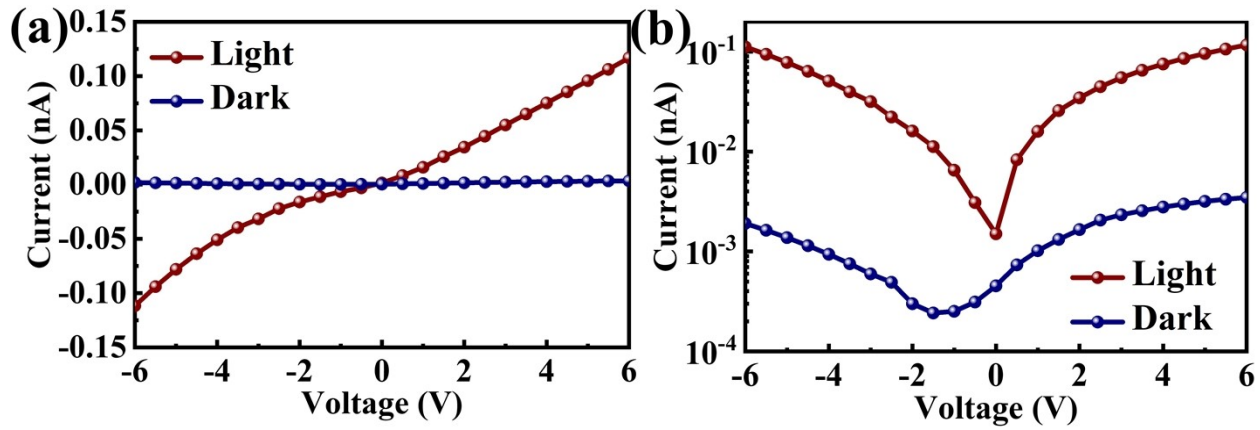

Figure S12. Current voltage (*I-V*) curves of the Sb_2S_3-H_2/Ar rod photodetector devices measured under dark and illumination with a 560 nm monochromatic light at a light intensity of 110 μW/cm^2, respectively.

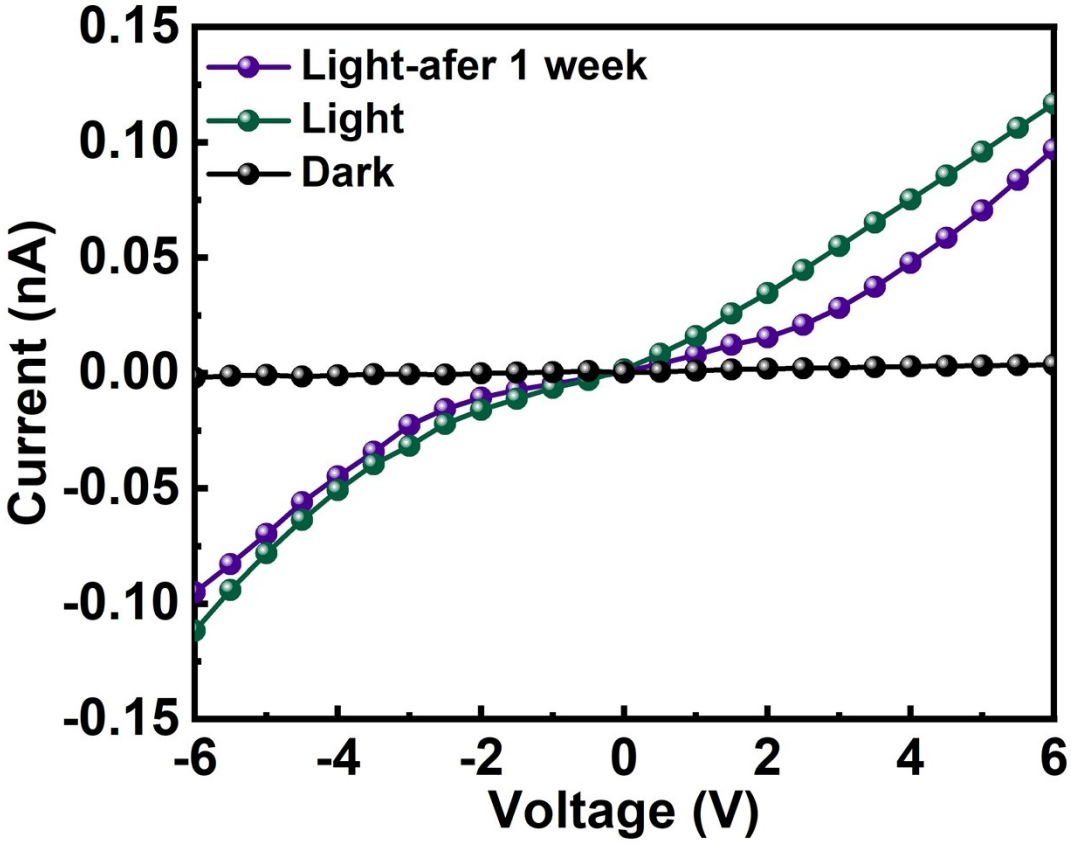

Figure S13. *I-V* curves of the Sb_2S_3-H_2/Ar rod photodetector device under dark and illumination of 110 μW/cm^2, respectively. It is noted that the photocurrent of the device after storage in air for 1 week decreases slightly compared to the fresh one.